DOI 10.1007/s11204-022-09772-0
Soil Mechanics and Foundation Engineering, Vol. 58, No. 6, January, 2022 (Russian Original No. 6, November-December, 2021)

UNDERGROUND STRUCTURES

EFFECTS OF LARGE-SCALE TWIN TUNNEL EXCAVATION ON AN EXISTING PILE GROUP: THREE-DIMENSIONAL CENTRIFUGE MODELING

UDC 624.154.7

Yuting Zhang,[1, 2] Chu Ding,[3] Hu Lu,[4]* and Wendong Ji[2]

[1]Tianjin University, Tianjin, China; [2]Tianjin Research Institute for Water Transport Engineering, Tianjin, China; [3]Key Laboratory of Geomechanics and Embankment Engineering of the Ministry of Education, Geotechnical Research Institute, Hohai University, Nanjing, China; [4] Shenzhen Polytechnic, Shenzhen, China,
* Corresponding author Email: lvhu1212@163.com.

Existing piles are commonly encountered during tunnel construction in congested underground areas. Tunnel-soil-pile interaction has recently attracted considerable research attention; however, previous studies have mainly focused on the pile response owing to small-scale tunnel excavation. In this study, we conducted a three-dimensional centrifuge test to investigate the deformation mechanisms of a pile group owing to large-scale twin tunnel excavation. Pile group settlement increases almost linearly with tunnel advancement in response to a decrease of the tunneling-induced stress. A shorter distance between the monitoring point and new tunnel results in higher pile group settlement. A maximum pile group settlement of 0.23% of the tunnel diameter (D) is observed directly above the tunnel centerline upon completion of a single tunnel excavation. After twin tunnel excavation, the maximum pile group settlement increases to 0.32% D and the location of the maximum pile group settlement shifts to the centerline between the two tunnels. As the tunnel face approaches the monitoring section, the existing pile group tilts rapidly toward the tunnel face. Tilting of the existing pile group decreases as the tunnel face passes through the monitoring section. The measured tilting of the pile group reaches a maximum when the tunnel face is located directly beneath the monitoring section. This demonstrates the three-dimensional deformation mechanisms of the pile group owing to tunnel excavation. If the tunnel excavation is simplified to a two-dimensional problem, tilting of the pile group along the longitudinal tunnel direction is ignored, which is on the nonconservative side.

Introduction

Metro tunnels have become an effective way to relieve traffic jams in response to the rapid development of urban modernization [1-2]. Existing piles are commonly encountered during tunnel construction in congested urban cities. Field studies have been conducted to explore the effects of tunnel construction on existing piles to ensure the long-term serviceability of pile-supported structures [3-5]. For example, tunnel excavation-induced ground loss reduces the bearing capacity of existing piles [3]. As a result of tunnel excavation, negative skin friction occurs at the bottom of the pile, which can have adverse effects on the pile bearing capacity [4].

Numerous centrifuge tests have been conducted to investigate tunnel-soil-pile interaction problems [6-10]. When the tunnel centerline is at or near the end of a pile, tunnel excavation induces a significant bending moment and lateral displacement in the existing piles, and changes in the axial force of the piles are significantly affected by the construction of a tunnel below the pile tip [6]. Jacobsz [7] conducted centrifuge tests in dry sand and identified an influence zone where large settlement is induced in the existing pile foundation. Lee and Chiang found that an end-bearing reduction caused excessive additional pile settlement owing to near-pile tunneling [8]. On the basis of centrifuge test results, Ong [9] found that additional tunneling-induced bending moments and axial forces of the piles are significantly affected by the pile head constraint conditions. Ma et al. [10]

Translated from Osnovaniya, Fundamenty i Mekhanika Gruntov, No. 6, November-December, 2021.

0038-0741/22/5806-0500 © 2022 Springer Science+Business Media, LLC

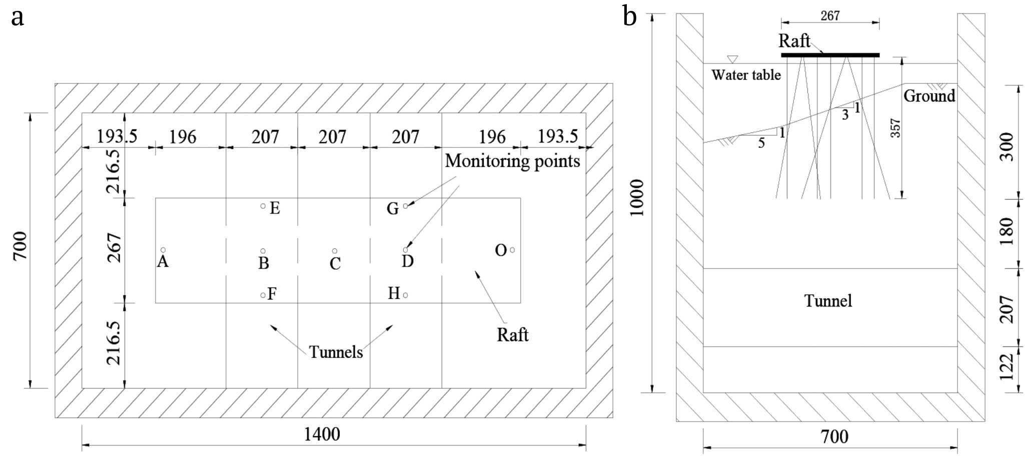

Fig. 1. Centrifuge model: a) plan view and b) elevation view (units: mm).

found that tunneling-induced bending moments in rear piles are considerably smaller than those in front piles owing to shielding effects provided by the latter. Several studies have been conducted to investigate the response of a single pile and pile group owing to twin tunnel excavation in dry sand [11-15].

Although several studies have investigated pile responses owing to tunnel excavation using centrifuge tests, most focused on the pile response in sand. Moreover, previous studies mainly simulated the construction of small-diameter (e.g., 6 m) metro tunnels, whereas the effects of large-scale (e.g., 15.3 m) twin tunnel excavation on pile response have been scarcely evaluated. In this study, we conducted a three-dimensional (3D) centrifuge test to investigate the deformation mechanisms of a pile group owing to twin tunnel excavation in sand and clay.

Three-Dimensional Centrifuge Modeling

We conducted a 3D centrifuge model test at the geotechnical centrifuge facility of the Tianjin Research Institute for Water Transport Engineering. The centrifuge had a rotating radius of 5 m, load capacity of 500 gt, and maximum acceleration of 250*g*. The 3D model container had a length of 1,400 mm, width of 1,000 mm, and depth of 1,000 mm. By considering the size of the model container and twin tunnels, the centrifugal acceleration was set to 75*g*. The scaling factors relevant to the centrifuge test are summarized in [16-18].

Figure 1 shows the plan and elevation views of the centrifuge model. Twin parallel large-scale tunnels were constructed underneath the Yangtze River. Prior to tunnel excavation, there was an operating pile-supported wharf. Additional settlement was inevitably induced in the pile foundation during construction of the two parallel tunnels. The burial depth (C) and outer diameter (D) of the new tunnels were 480 and 207 mm, respectively, corresponding to 36 and 15.5 m in the prototype. The cover-to-tunnel diameter ratio (C/D) was 2.3. The clearest distance between the two horizontally parallel tunnels was 207 mm; equivalent to 15.5 m in the prototype ($1D$). The maximum thickness of the soil simulated in the test was 810 mm, corresponding to 60.75 m in the prototype. The ground was simulated with two slopes of 1:3 and 1:5, according to the site investigation.

The current pile support wharf was scaled down to model size based on the relevant scaling laws. This consisted of a raft and several piles. Bolts were used to connect the raft and piles. An aluminum alloy plate with dimensions of 1,013 × 267 × 10 mm was used to simulate the raft. The twin tunnels were constructed directly underneath the pile foundation with a clear distance of 180 mm; equivalent to 13.5 m in the prototype.

TABLE 1

Soil type	Thickness in model scale (mm)	Unit weight (kN/m^3)	Cohesion (kPa)	Frictional angle (°)	Compression modulus (MPa)
Silty clay	217	18.8	3.2	22.8	8.2
Sand	200	19.5	0.0	36.0	10.9
Silty clay	173	18.8	3.2	22.8	8.2
Sand	225	19.5	0.0	36.0	10.9

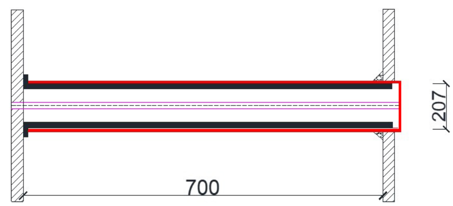

Fig. 2. Simulation of tunnel excavation (units: mm).

Testing materials

According to the site investigation, the soil underneath the Yangtze River mainly consists of silty clay, fine sand, sandy clay, and coarse sand. In this test, the soil ground was simplified to four layers consisting of two silty clay and two sand layers. Fujian standard sand and silty clay were used to prepare the sand and clay samples, respectively. Because soil-structure interactions are strongly affected by soil parameters [1-2, 15], additional laboratory tests were conducted to determine the sand and clay sample parameters. The internal friction angle and compression modulus of the sand and silty clay were determined based on triaxial shear tests and compression tests. The soil properties are summarized in Table 1.

The pile group consisted of 10 rows of 5 straight piles and 4 inclined piles for a total of 90 piles. In the field, the wharf was supported by a pre-stressed square pile with a side length of 550 mm. Circular tubes with an outer diameter of 9.2 mm and thickness of 0.8 mm (in model scale) were used to simulate the model piles based on the flexural stiffness. The lengths of the straight and inclined piles were 357 and 370–378 mm in model scale, respectively.

Tunnel excavation simulation

Previous studies have simulated tunnel excavation by draining water from cylindrical rubber bags [10-14, 16]. This method cannot simulate friction between the shield and soil during tunnel advancement. To overcome those shortcomings, we developed a new tunnel excavation technique.

Figure 2 shows a cross-section view of the tunnel excavation simulation system. The tunnel model mainly consisted of a newly built tunnel, a stainless steel sleeve, and a tunnel support system. The newly built tunnel was located inside the stainless steel sleeve. The thickness of the sleeve was used to control tunnel volume loss. During the centrifuge test, the newly built tunnel was fixed and the sleeve was pushed away from the new tunnel to simulate tunneling-induced volume loss. In this study, the outer diameters of the newly built tunnel and stainless steel sleeve were 207 and 209 mm, respectively. This means that the sleeve thickness was 1 mm in model scale. Pushing the stainless steel sleeve away from the newly built tunnel resulted in the simulation of 1% tunnel volume loss. Because the sleeve was made of a rigid material, the tunnel shape was circular after tunnel construction. Furthermore, pushing the sleeve simulated the friction effects between the shield shell and soil, which is more consistent with that in practice.

Nine displacement sensors were installed in the centrifuge test. As shown in Fig. 1a, five linear variable differential transformers (LVDTs) were installed to measure settlement of the pile group

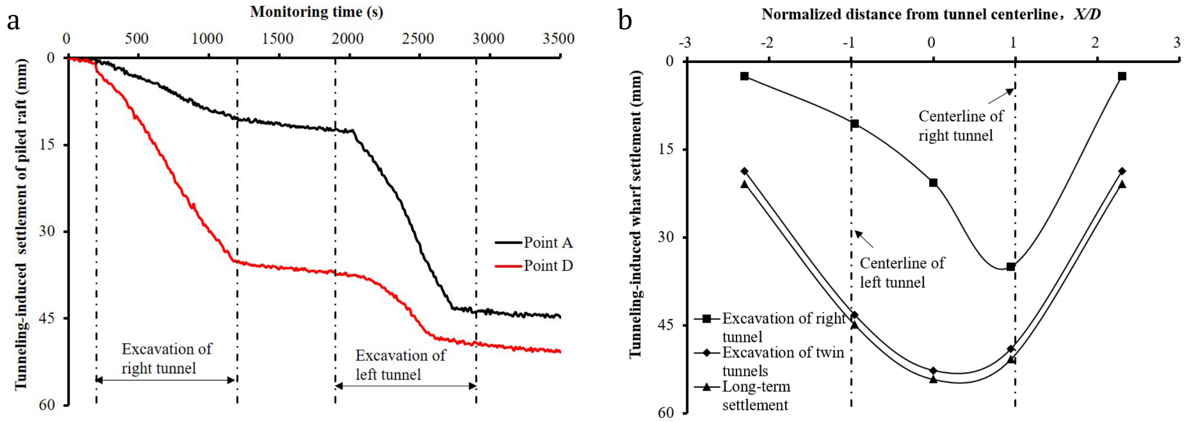

Fig. 3. Measured settlement of the piled raft: a) during tunnel excavation, b) along the tunnel transverse direction.

along the transverse tunnel direction. Four laser sensors were installed to measure pile group settlement along the longitudinal tunnel direction. The pile group tilting was obtained based on the measured settlement along the longitudinal tunnel direction. The accuracy of the LVDTs and laser sensors was 0.02 mm.

After installing a drainage pipe at the bottom of the model container, the sandy layer was prepared using the sand pluvial deposition method. The raining distance between the sand hopper and sand surface was held at 700 mm to reach the designed sand density. After preparing the sandy layer, silty clay was prepared layer by layer according to the designed density. Upon completion of each clay layer, the clay layer surface was scraped to increase the contact between layers. To saturate the soil sample, deaired water was slowly injected from the bottom of the model box, and the soil sample was soaked for 24 h. A vacuum was applied at the top of the model box to ensure a high degree of saturation.

Testing procedure

The centrifuge testing procedure was divided into the following stages.

1. The acceleration of the centrifuge was gradually increased to 75*g* over approximately 10 min.
2. The centrifuge was run at 75*g* for 10 h to complete the primary consolidation.
3. After the transducer readings stabilized, the stainless steel sleeve of right tunnel was gradually pushed out. The excavation of the second tunnel was then simulated using the same method over a period of approximately 20 min.
4. The centrifuge was gradually reduced to 1*g* over a period of approximately 30 min.

Intepretation of Centrifuge Test Results

Figure 3a shows the typical variation of pile group settlement during tunnel construction. Pile group settlement increases almost linearly with tunnel advancement. Points A and B are located above the left and right tunnels, respectively. The excavation of the right tunnel was conducted first, followed by excavation of the left tunnel. During the excavation of the right tunnel, the settlement measured at point A was significantly smaller than that measured at point D. The measured settlements at points A and D were 10.8 and 35.3 mm, respectively. Pile group settlement then continued to increase after completion of the right tunnel excavation owing to the dissipation of excess pore water pressure. During excavation of the left tunnel, the incremental pile group settlement measured at point A was significantly larger than that at point D. The corresponding incremental settlement at points A and D were 30.1 and 11.7 mm, respectively. A shorter distance between the monitoring point and newly constructed tunnel resulted in substantially higher pile group settlement. Tunneling-induced settlement of the pile group is therefore closely related to the relative position between the tunnel and pile.

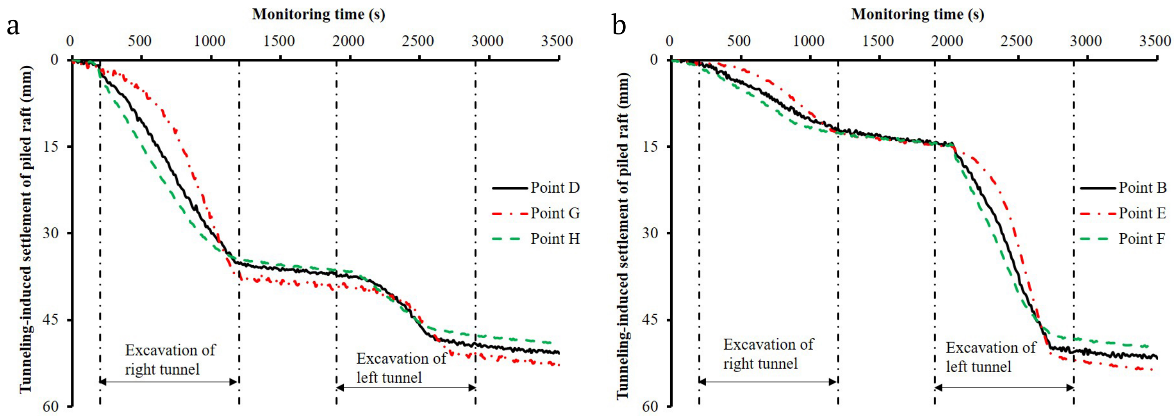

Fig. 4. Variation of the measured settlement of the piled raft with constuction time: a) centerline of the right tunnel, b) centerline of the left tunnel.

Figure 3b shows the measured pile group settlement along the transverse tunnel direction. Upon completion of the right tunnel, the settlement of the pile group above the right tunnel was substantially more than that above the left tunnel. Owing to the stress relief resulting from the right tunnel excavation, a maximum pile group settlement of 35 mm (i.e., 0.23% *D*) was observed above the tunnel centerline. The measured pile group settlement decreased with increasing distance between the monitoring point and tunnel centerline. During construction of the left tunnel, the pile group settlement increased rapidly. After the twin tunnels were constructed, the settlement profile of the pile group became symmetrical. The maximum settlement increased to 49 mm (0.32% *D*), and the location of the maximum pile group settlement shifted to the centerline between the two tunnels. Two months after tunnel construction, the maximum pile group settlement had increased to 50.8 mm (an increase of 3.7%) owing to the dissipation of excess pore water pressure. Since the settlement of pile group is closely related to soil properties [19], countermeasures such as soil treated by bacteria may be used to alleviate tunneling-induced the settlement of pile group [20].

Figure 4 shows the variations of measured pile group settlement along the longitudinal tunnel direction. The right and left tunnels were driven from points H to G and F to E, respectively. Settlement was observed at all of the monitoring points during the excavation of both tunnels. As the tunnel face approached the monitoring section, settlement differences between points H and G increased. However, these differences decreased as the tunnel face extended beyond the monitoring section. The variation of settlement with tunnel advancement at points F and E was the same as that of points H and G. Upon completion of the twin tunnel excavation, the differences between pile group settlement along the longitudinal direction was less than 8%.

Tilting of the pile group was calculated based on the measured settlement along the longitudinal tunnel direction. Figure 5 shows the longitudinal tilting of the pile group during the twin tunnel excavation. As the right tunnel face approaches the monitoring section, the existing pile group tilted toward the tunnel face and the tilting rapidly increased. This is because tunnel excavation reduced the stress ahead of the tunnel face. As the tunnel face passed through the monitoring section, tilting of the existing pile group decreased. This is because the stress reduction became symmetrical with respect to the monitoring section. Additionally, the tilting of the pile group above the left tunnel initially increased followed by a decrease with progressing tunnel advancement. However, the measured tilting above the left tunnel was substantially smaller than that above the right tunnel during excavation of the right tunnel. This is because the monitoring points above the left tunnel were located far from the right tunnel face. The same was observed during construction of the left tunnel;

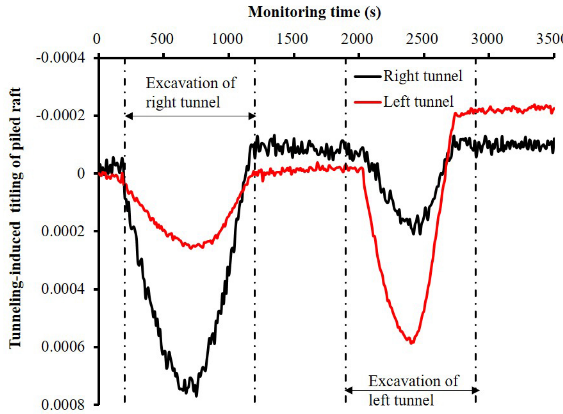

Fig. 5. Tunneling-induced tilting of the piled raft.

however, the incremental tilting of the pile group above the left tunnel was much larger than that above the right tunnel. This further demonstrates that the response of the piled raft is closely related to the relative position of the tunnel and pile. During the excavation of both tunnels, the measured tilting above the twin tunnels reached a maximum value when the tunnel face was located directly beneath the monitoring section. This clearly demonstrates the 3D deformation mechanisms of the pile group owing to tunnel excavation. If tunnel excavation is simplified to a two-dimensional problem (i.e., simulated in a single step), the longitudinal tilting of the pile group is ignored, which is on the unconservative side. This highlights the importance of simulating tunnel excavation in 3D physical and numerical models.

Conclusions

1. The measured settlement of the pile group increased almost linearly with tunnel advancement owing to a reduction of tunnel excavation-induced stress. Tunneling-induced settlement of the pile group is closely related to the relative position between the tunnel and pile. A shorter distance between the monitoring point and tunnel construction results in larger pile group settlement.

2. After a single tunnel excavation, a maximum pile group settlement of 0.23% *D* was observed above the tunnel centerline. Upon completion of the twin tunnel excavation, the maximum pile group settlement increased to 0.32% *D* and the location of the maximum surface settlement shifted to the centerline between the two tunnels.

3. As the right tunnel face approached the monitoring section, the existing pile group tilted rapidly toward the tunnel face. As the tunnel face passed through the monitoring section, the tilting of the existing pile group decreased. This is because the stress reduction became symmetrical with respect to the monitoring section. During tunnel advancement, the measured tilting above the twin tunnels reached a maximum when the tunnel face was located directly beneath the monitoring section. This clearly demonstrates the 3D deformation mechanisms of the pile group owing to tunnel excavation. Pile group tilting along the longitudinal direction is ignored when tunnel excavation is simplified to a two-dimensional problem, which is on the unconservative side.

Acknowledgment

This work was supported by the Fundamental Research Funds for the Central Public Welfare Research Institutes (No. tks190203) and the Characteristic Innovation Project of Department of Education of Guangdong Province, China (2019GKTSCX087).

References

1. J. W. Shi, C. W. W. Ng, and Y. H. Chen, "A simplified method to estimate three-dimensional tunnel responses to basement excavation," *Tunn. Undergr. Sp. Tech.*, **62**: 53-63 (2017).
2. J. W. Shi, Y. Wang, and C. W. W. Ng, "Numerical parametric study of tunneling–induced joint rotation angle in jointed pipelines," *Can. Geotech. J.*, **53**(12): 2058-2071 (2016).
3. S. W. Jacobsz, "*The effects of tunneling on piled foundations*," Ph.D. thesis, University of Cambridge, Cambridge, UK (2002).
4. X. J. Yang, F. H. Deng, W. Nie, and G.G Li, "Study on effect of metro tunneling on carrying capacity of pile foundation," *Chin. J. Rock Mech. Eng.*, **25**, 1290-1295 (2006).
5. Z. Li and M. S. Huang, "Analysis of settlement and internal forces of group pile due to tunneling," *Chin. J. Geotech. Eng.,* **29**, 398-402 (2007).
6. N. Loganathan, H. G. Poulos, and D. P. Stewart, "Centrifuge model testing of tunnelling-induced ground and pile deformations," *Geotechnique*, **50**(3), 283-294 (2000).
7. S. Jacobsz, J. Standing, R. Mair, T. Hagiwara, and T. Sugiyama, "Centrifuge modeling of tunneling near driven piles," *Soils Found.*, **44**(1), 49-56 (2004).
8. C. J. Lee and K. H. Chiang, "Responses of single piles to tunneling-induced soil movements in sandy ground," *Can. Geotech. J.*, **44**(10), 1224-1241 (2007).
9. C. W. Ong, "Centrifuge model study of tunnel-soil-pile interaction in soft clay," Ph.D. thesis, National University of Singapore, Singapore (2009).
10. S. K. Ma, H. Lu, K. S. Wong, C. W. W. Ng, and N. F. Zhao, "Three-dimensional centrifuge modelling of the effects of twin tunnelling on existing pile group in expansive clay," *Chin. J. Geotech. Eng.*, **35**, 1337-1342 (2013).
11. A. M. Marshall and R. J. Mair, "Tunneling beneath driven or jacked end bearing piles in sand," *Can. Geotech. J.*, **48**(12), 1757-1771 (2011).
12. C. W. W. Ng and H. Lu, "Effects of construction sequence of twin tunnelling at different depth on a single pile," *Can. Geotech. J.*, **51**(2), 173-183 (2013).
13. C. W. W. Ng, H. Lu, and S. Y. Peng, "Three-dimensional centrifuge modelling of twin tunnelling effects on an existing pile," *Tunn. Undergr. Sp. Tech.*, **35**, 189-199 (2013).
14. Y. Hong, M. A Soomro, and C. W. W. Ng, "Settlement and load transfer mechanism of a pile group due to side-by-side twin tunnelling," *Comput. Geotech.*, **64**, 105-119 (2015).
15. J. W. Shi, J. Q. Wei, C. W. W. Ng, and H. Lu, "Stress transfer mechanisms and settlement of a floating pile due to adjacent multi-propped deep excavation in dry sand," *Comput. Geotech.*, **116**, 103216 (2019).
16. J. W. Shi, Y. Wang, and C. W. W. Ng, "Three-dimensional centrifuge modeling of ground and pipeline response to tunnel excavation," *J. Geotech. Geoenviron. Eng.*, **142**(11), 04016054 (2016).
17. J. W. Shi, Z. Z. Fu, and W. L. Guo, "Investigation of geometric effects on three-dimensional tunnel deformation mechanisms due to basement excavation," *Comput. Geotech.*, **106**, 108-116 (2019).
18. W. Shi, C. Ding, C. W. W. Ng, H. Lu, and L. Chen, "Effects of overconsolidation ratio on tunnel responses due to overlying basement excavation in clay, " *Tunn. Undergr. Sp. Tech.*, **97**, 103247 (2020).
19. S. Yang, B. Leshchinsky, K. Cui, F. Zhang, and Y.F. Gao, "Influence of failure mechanism on seismic bearing capacity factors for shallow foundations near slopes," *Geotechnique*, DOI: http://doi.org/10.1680/jgeot.19.P.329 (2020).
20. J. He, Y.F. Gao, Z.X. Gu, J. Chu, and L.Y. Wang, "Characterization of crude bacterial urease for $CaCO_3$ precipitation and cementation of silty sand," *J. Mater. Civil Eng.*, **32**(5), 04020071 (2020).